Research Reports

Title: Size and shape variability in human molars during odontogenesis

Abstract

Under the patterning cascade model (PCM) of cusp development inspired by developmental genetic studies, it is predicted that the location and the size of later-forming cusps are more variable than those of earlier-forming ones. Here we assessed whether differences in the variability among cusps at total and each particular crown components (enamel-dentin junction [EDJ], outer enamel surface [OES], and cement-enamel junction [CEJ]) could be explained by the PCM, using human maxillary permanent first molars (UM1) and second deciduous molars (um2). Specimens were μCT-scanned, and 3D models of EDJ and OES were reconstructed. Based on these models, landmark-based 3D geometric morphometric analyses were conducted. Size variability in both tooth types was generally consistent with the above prediction, and the differences in size variation among cusps were smaller for the crown components that are completed in later stages of odontogenesis. With a few exceptions, however, the prediction was unsupported regarding shape variability, and UM1 and um2 showed different patterns. Our findings suggested that the pattern of size variability would be caused by temporal factors such as the order of cusp initiation and the duration from the beginning of mineralization to the completion of crown formation, whereas shape variability may be affected by both topographic and temporal factors.

Introduction

In multicuspidate teeth, secondary enamel knots appear sequentially at the future location of each cusp and repeatedly use the same signaling pathways (Jernvall and Jung, 2000). The spatial patterning and number of cusps are determined by the iterative activation of secondary enamel knots and by reciprocal signaling within and between oral epithelium and mensenchyme (Patterning Cascade Model: PCM; Jernvall, 2000). In this model, cusp initiation is sequential, and the location and size of later-forming cusps are influenced by those of earlier-forming ones (Salazar-Ciudad *et al.*, 2003).

If the positioning of later-forming secondary enamel knots is dependent on the positioning of the pre-existing secondary enamel knots and if the perturbations in earlier cascade events are amplified in later events, it is very likely that the variation of the morphology of later-forming cusps will surpass that of early-forming cusps (Jernvall, 1997; Polly, 1998). This prediction was supported concerning the cusp height and position in seal dentition (Jernvall, 1997, 2000), and also received support from studies of cusp size variability (Townsend *et al*., 2003; Harris and Dihn, 2006; Takahashi *et al*., 2007) and Carabelli cusp expression (Hunter *et al.*, 2010) in the human molars. However, Polly (1998) found that earlier-forming cusps were more variable in their positions than later-forming cusps in viverravid molar, and proposed that the order of cusp initiation and the timing of the termination of intercusp growth determine patterns of variability in cusp position and height. Polly (1998) mentioned the possibility that initial difference in variability among cusps might be obliterated in human molar that had a long gap between cusp initiation and the termination of intercusp growth because developmental perturbations could have a cumulatively greater effect on earlier-forming cusps.

To understand the precise variability-generating mechanisms regulated by the PCM, it is necessary to obtain detailed information about differences of morphological variability among cusps, about which there remains a dearth of information. For example, except for the spatial distribution of cusp tips in mammalian molars (Jernvall, 1997, 2000; Polly, 1998), little attention has been paid to cusp *shape* variability. Previous studies have principally focused on the outer enamel surface (OES) morphology of the occlusal surface (Corruccini, 1979; Harris and Dihn, 2006; Takahashi *et al.*, 2007). The results obtained could be explained by the PCM that morphological variability becomes larger in the later-forming cusps. However, the PCM would relate more directly to cusp patterning at EDJ

(Skinner and Gunz, 2010) than to the other parts of crown components – OES-ridge, OES-circumferences, and cement-enamel junction (CEJ) – that are elaborated through the subsequent developmental processes, including enamel matrix deposition and the elongation of cervical loop (Butler, 1956; Jernvall and Jung, 2000). Could differences in the variability among cusps at total and each particular crown components be explained by the PCM? Comparing morphological variability among cusps at these components could provide significant information about the variability-generating mechanisms during odontogenesis, which would be relevant to morphological evolution because developmental process structures morphological variation on which natural selection can act, which biases the developmental processes available for subsequent generations.

Here, we examined the pattern of morphological variability among cusps of the maxillary permanent first molar (UM1) and second deciduous molar (um2). They have similar main-cusp and occlusal groove patterns and belong to the same molarization field (Butler, 1967), which does not contradict recent findings of molecular, cellular or genetic studies (Sharpe, 1995; Mitsidis and Smith, 2006). Although UM1 and um2 share similar patterns of occlusal morphology, UM1 is larger than um2 in size. Additionally, um2 crown is initiated 12.5-19 weeks after fertilization and is completed by 11 months after birth, whereas UM1 crown begins to calcify at birth and is completed at 2.6-2.7 years (TenCate, 2012). Thus, developmental timing, period, and rate are distinct between UM1 and um2, which enables us to explore their effects on patterns of morphological variability. Specifically, we tested the following hypotheses.

Hypothesis 1: later-forming cusps have greater *size variability* than earlier-forming ones, and this holds for each crown component (EDJ-ridge, OES-ridge, OES-circumferences, and CEJ).

Hypothesis 2: the *shape variability* of later-forming cusps is greater than that of earlier-forming ones, and this holds for each crown component.

Hypothesis 3: UM1 and um2 share common patterns of size and shape variability for each crown component.

Materials and Methods

The samples used in this study comprised fully formed but unworn UM1 and um2 crowns obtained from archaeological sites in Japan. The total sample (57 UM1 and 48 um2) consisted of samples from the Jomon (14500-300 BC; n=8 and 5), Medieval (13-15C AD; n=13 and 8), and Edo (17-19C AD; n=36 and 35) periods. Although the total sample was from a mixture of populations from different periods and regions, the aim of this study was to investigate differences and patterns of variability produced by a common tooth formation process of the Holocene human, and mixing these samples does not violate the objective of this study. No discrimination between right and left teeth was made to maximize sample size, but only a single tooth was used from each individual. All specimens were regarded as left side. Right molar μCT-images were transformed into the mirror image using ImageJ software (NIH, USA). Sex was unknown for most of the samples, since they were taken from juvenile individuals.

Each specimen was scanned using a μCT scanner (ScanXmateA080S, Comscantecno, Japan) with a pixel size and slice interval of 31‑32 μm (80 kV, 125 μA). To facilitate tissue segmentation, the image stack for each tooth was filtered using a median filter followed by a kuwahara filter, and enamel and dentin tissues were segmented by the seed region growing method in ImageJ. Triangular mesh models of the 3D EDJ and OES of each specimen were reconstructed using Analyze 6.0 (Mayo Clinic, USA) with the marching cube method. Subsequent procedures were done using the software Rapidform 2004 (INUS Technology, Korea).

We digitized each main cusp (paracone, protocone, metacone, and hypocone) region of four crown components (EDJ-ridge, OES-ridge, OES-circumferences, and CEJ) in a tooth (more details in Supplement file). The dataset was represented by four coordinate matrices comprising a total of 8 landmarks and 84 semi-landmarks (Figure 1A-B).

Centroid size (CS) was calculated in particular components of cusps. Coefficient of variation (CV) of the CS was used to compare size variability, and tested as suggested by Sokal and Braumann (1980).

For comparison of shape variability among cusps, Generalized Procrustes Analysis (GPA; Rohlf and Slice, 1990) was performed using MorphoJ version 1.05d (Klingenberg, 2011). To include the information of relative spatial distribution among cusps, GPA was repeated for the landmark set of the total and each crown component. The square root of the sum of the squared distances between

Procrustes transformed coordinates of each cusp and its landmark mean configuration was used as the measure of shape variability (Polly, 1998; Jernvall, 2000). To test whether there was a significant difference in variation among cusps, a nonparametric Kruskall-Wallis test and multiple-comparison test were performed. The correlation between the shape variability and the order of cusp initiation (paracone, protocone, metacone, and hypocone: Turner, 1963; Kraus and Jordan, 1965) was assessed using Spearman's rank coefficient. All statistical analyses were performed using R version 2.13.1 (R Development Core Team, 2011), with statistical significance set at $P<0.05$.

Results

Hypothesis 1 (greater size variability in later-forming cusps).

The CV of total crown components of UM1 did not show any significant difference, although the last-forming hypocone had a somewhat greater variation (Figure 1C). For EDJ-ridge, the hypocone had a larger CV than the other cusps ($P=0.074$). For OES-ridge, the hypocone showed higher variability than the other cusps, but the difference in variability was not significant ($P= 0.397$). For OES-circumferences, earlier-forming cusps showed slightly higher variability, but the difference among cusps was not significant ($P=0.895$). For CEJ, the later-forming metacone was more variable, but there was not significant difference among cusps ($P=0.430$). In summary, hypothesis 1 was unsupported in UM1, but there was a tendency of higher size variability in later-forming cusps for EDJ-ridge.

The difference in size variation among cusps was pronounced in um2 (Figure 1D). For every topological feature except CEJ, the hypocone showed significantly higher variability than other cusps. In the case of CEJ, although the hypocone tended to be more variable, no significant difference was observed ($P=0.169$), and the difference among cusps was smaller than that for other parts of the crown components.

Hypothesis 2 (greater shape variability in later-forming cusps).

In UM1, a negative correlation was observed between shape variability and the cusp initiation order for OES-circumferences ($P<0.001$) and CEJ ($P=0.026$) (Figure 2). No correlation existed for other components. In the case of OES-circumferences, a nonparametric multiple-comparison test showed that the hypocone was significantly less variable in shape than the paracone (*P*=0.028) and protocone (*P*=0.030). In the case of CEJ, the metacone was less variable than the paracone (*P*=0.014). These results did not support hypothesis 2, and were also inconsistent with the order of cusp initiation.

In um2, a positive correlation was observed between shape variability and the cuspal initiation order for total crown components (*P*=0.010) and OES-ridge (*P*=0.004) (Figure 3). Direct comparisons of total crown components revealed that the hypocone was more variable than the paracone (*P*=0.018). Moreover, for OES-ridge, Kruskall-Wallis analysis revealed significant difference among cusps (*P*=0.031), and the paracone was less variable than the hypocone (*P*=0.048). For CEJ, there was significant difference among cusps (*P*=0.016), and the metacone was less variable than the protocone (*P*=0.058), although the correlation with the order of cusp initiation was not significant (*P*=0.554). As a whole, lingual cusps (protocone and hypocone) were more variable than buccal cusps (paracone and metacone). Therefore, hypothesis 2 was supported only for total crown components and OES-ridge.

Hypothesis 3 (UM1 and um2 share common patterns of size and shape variability).

As noted above, the tendency of greater size variability of later-forming cusps at least in EDJ was common between UM1 and um2, whereas the shape variability showed a tooth-specific pattern. Then, hypothesis 3 was supported only partially for size variability, and was refuted for shape variability.

Discussion

Human molars grow substantially after the cusps form, and then this growth might hide any small differences in cusp height and size (Butler, 1956). However, recent developmental analysis revealed that crown sizes were regulated by intrinsic factors from mesenchymal tissues (Cai *et al*., 2007). Because the secondary enamel knots are induced in a sequential cascade, when a broader inhibition field which is controlled by the nested expression and interaction of activator and inhibitor proteins (Jernvall and Jung, 2000) around earlier-forming enamel knot increases cusp spacing, later-forming cusps will be smaller and *vice versa*. Therefore, it is expected that the size of earlier-forming cusps will be larger at the expense of the later-forming cusps if the rate of formation of the earlier-forming cusps is faster and/or the duration of their formation is longer than those of the later-forming cusps (Takahashi *et al*., 2007). This causes relatively larger size variability in later-forming cusps, which can be observed in not only OES but also various parts of the crown components albeit mineralization process does not interact across cusps.

Temporal factors during odontogenesis, such as the order of cusp initiation and the duration from the beginning of mineralization to the completion of crown formation, are likely responsible for the pattern of size variability. The differences in size variation among cusps are greater in the earlier-forming crown components (in particular EDJ-ridge) and the influence of the order of cusp initiation is smaller in the later-forming components. UM1 and um2 differ regarding how much and how long the later-forming cusps are susceptible to variability in size. The difference in variability among cusps in um2 is greater than that in UM1, and it is preserved in the later phase of development. Because the developmental period of UM1 is longer than that of um2 (Liversidge and Molleson, 2004), the relatively large size variability of earlier-forming cusps in UM1 probably results from greater cumulative perturbation over a longer period of odontogenesis, whereas the relatively shorter developmental period of um2 leads to the lasting effect of the order of cusp initiation. Polly (1998) stressed that initial differences in height and variability among cusps might be erased when there was a long delay between the enamel knot activation and the intercusp growth termination. The present study suggests that this idea may be applicable to the whole process of the odontogenesis. Apart from temporal factors for size variability, natural selection on occlusion can cause smaller variability of earlier-forming cusps consisted of the trigon, which might explain clearer tendency at EDJ and OES which are more responsible for occlusion and in um2 which preserves primitive morphology (Butler, 1956).

Unlike size variability, shape variability in UM1 did not show patterns consistent with the PCM-based hypothesis of greater variability in later-forming cusps. Rather, the earlier-forming cusps were more variable than the later-forming cusps regarding OES-circumferences and CEJ, which could be explained by applying Polly's (1998) previously mentioned idea. The greater variability of the earlier-forming cusps reflects a greater effect of cumulative perturbation due to the longer period of development. However, there was no significant difference between the later-forming and earlier-forming cusps regarding variability in shape during the earlier stage of odontogenesis. This might be the result of complicated effects of the order of cusp initiation, cumulative perturbations of the longer developmental period, and/or unknown developmental factors.

The patterns of shape variability of um2 were consistent with the order of cusp initiation for OES-ridge, but not for EDJ-ridge. In the case of EDJ-ridge, the hypothesized pattern might have been erased by multifactorial effects during development. The pattern of shape variability of the later-forming OES-ridge might result from the order of cusp initiation amplified by enamel deposition. In the later stage of odontogenesis, the shape of lingual cusps is more variable than that of buccal ones. This may be explained by several developmental factors, such as the lingual side-dominated growth pattern, the spatial relationship with the surrounding tissues including maxillary bone and/or other tooth germs, and the available space for tooth growth (Boughner, 2011), which might have more influence on the patterns of shape variability, than the effect of cumulative perturbation due to the longer period of development.

The size variability of human molar cusps follows the theoretical explanations proposed by Jernvall (2000). However, with a few exceptions, the hypothesized variability pattern was not observed regarding cusp shape variability, and instead, UM1 and um2 showed different patterns of shape variability from each other. During odontogenesis, temporal factors would contribute to the patterns of size variability, whereas shape variability might be more influenced by topological factors.

Acknowledgements

The authors thank H. Ohshima for thoughtful advice, P. Gunz and P. Mitteroecker for permission to use software routines, and K. Hirata, K. Shimatani, and K. Miyazawa for access to specimens. This study was supported in part by JSPS Research Fellowship (11J00940), and by Grants for Excellent Graduate Schools, MEXT, Japan. The authors declare no potential conflicts of interest with respect to the authorship and/or publication of this article.

Figure legends

Figure 1. Digital image of maxillary permanent first molar crown (lingual view) and barplot of patterns of size variability. (A) OES-ridge curve and OES-circumferences digitized on the OES. (B) EDJ-ridge curve and CEJ curve digitized on the EDJ surface. Red circles are landmarks, yellow circles are semi-landmarks, and green rhomboids are breakpoints. pa, paracone; pr, protocone; me, metacone; hy, hypocone. (C) Barplot of patterns of size variability in UM1. (D) Barplot of patterns of size variability in um2. Significance tests for coefficients of variation for centroid size among cusps were performed following the recommendations of Sokal and Braumann (1980). There was a tendency of higher size variability in later-forming cusps, and the variability difference among cusps was smaller in the later-forming components.

Figure 2. Patterns of shape variability in UM1. Relationship between variability and cusp initiation order is shown for total crown components (A), EDJ-ridge (B), OES-ridge (C), OES-circumferences (D), and CEJ (E). Differences among cusps were tested by Kruskall-Wallis test, followed by nonparametric multiple-comparison test. R_s, Spearman's rank correlation coefficients; * $P<0.05$; ** $P<0.01$; *** $P<0.001$. The greater variability of the earlier-forming cusps was observed in the later-forming components.

Figure 3. Patterns of shape variability in um2. Relationship between variability and cusp initiation order is shown for total crown components (A), EDJ-ridge (B), OES-ridge (C), OES-circumferences (D), and CEJ (E). Differences among cusps were tested by Kruskall-Wallis test, followed by nonparametric

multiple-comparison test. R_s, Spearman's rank correlation coefficients; * $P<0.05$; ** $P<0.01$; *** $P<0.001$. Later-forming cusps showed greater varibility in total crown component and OES-ridge whereas lingual cusps showed greater variability in CEJ.

References

Boughner (2011) Making space for permanent molars in growing baboon (Papio anubis) and great ape (Pan paniscus and P. troglodytes) mandibles: Possible ontogenetic strategies and solutions. *Anat Res Int* http://dx.doi.org/10.1155/2011/484607.

Butler PM (1956). The ontogeny of molar pattern. *Biol Rev* 31: 30–70.

Butler PM (1967). Comparison of the development of the second deciduous molar and first permanent molar in man. *Arch Oral Biol* 12:1245–1260.

Cai J, Cho SW, Kim JY, Lee MJ, Cha YG, Jung HS (2007). Patterning the size and number of tooth and its cusps. *Dev Biol* 304:499–507.

Corruccini RS (1979). Molar cusp-size variability in relation to odontogenesis in hominoid primates. *Arch Oral Biol* 24:633–634.

Harris EF, Dinh DP (2006). Intercusp relationships of the permanent maxillary first and second molars in American whites. *Am J Phys Anthropol* 130:514–528.

Hunter JP, Guatelli-Steinberg D, Weston TC, Durner R, Betsinger TK (2010). Model of Tooth Morphogenesis Predicts Carabelli Cusp Expression, Size, and Symmetry in Humans. *Plos ONE* 5 e11844. doi:10.1371/journal.pone.0011844.

Jernvall J (1995). Mammalian molar cusp patterns: Developmental mechanisms of diversity. *Acta Zoologica Fennica* 198:1–61.

Jernvall J (1997). Developmental basis of mammalian molar cusp evolution. *J Vert Paleontol* 17(*Suppl*):56A.

Jernvall J (2000). Linking development with generation of novelty in mammalian teeth. *Proc Nat Acad*

Sci USA 97:2641–2645.

Jernvall J, Jung HS (2000). Genotype, phenotype, and developmental biology of molar tooth characters. *Year Phys Anthropol* 43:171–190.

Klingenberg CP (2011). MorphoJ: an integrated software package for geometric morphometrics. *Molec Ecol Res* 11:353–357.

Kraus BS, Jordan RE (1965). The Human Dentition Before Birth. Philadelphia:Lea and Febiger.

Liversidge HM, Molleson T (2004). Variation in crown and root formation and eruption of human deciduous teeth. *Am J Phys Anthropol* 123:172–180.

Mitsidis TA, Smith MM (2006). How do genes make teeth to order through development? *J Exp Zool* 306B: 177–182.

Polly PD (1998). Variability, selection, and constraints: development and evolution in viverravid (Carnivora, Mammalia) molar morphology. *Paleobiology* 24:409–429.

R Development Core Team. (2011) R: A Language and Environment for Statistical Computing. Version 2.13.1. http://cran.R-project.org. R Foundation for Statistical Computing, Vienna.

Rohlf FJ, Slice D (1990). Extensions of the Procrustes method for the optimal superimposition of landmarks. *Syst Zool* 39:40–59.

Salazar-Ciudad I, Jernvall J, Newman, SA (2003). Mechanisms of pattern formation in development and evolution. *Development* 130: 2027–2037.

Skinner MM, Gunz P (2010). The presence of accessory cusps in chimpanzee lower molars is consistent with a patterning cascade model of development. *J Anat* 217: 245–253.

Sharpe PT (1995). Homeobox genes and orofacial development. *Connect Tissue Res* 32: 17–25.

Sokal RR, Braumann CA (1980). Significance tests for coefficients of variation and variability profiles. *Syst Zool* 29:50–66.

Takahashi M, Kondo S, Townsend GC, Kanazawa E (2007). Variability in cusp size of human maxillary molars, with particular reference to the hypocone. *Arch Oral Biol* :52:1146–54.

TenCate AR (2012). Oral Histology: Development, Structure and Function, 8^{th} Edition. C.V. Mosby Company, St. Louis.

Townsend G, Richards L, Hughes T (2003). Molar intercuspal dimensions: genetic input to phenotypic variation. *J Dent Res* 82:350–355.

Turner EP (1963). Crown development in human deciduous molar teeth. *Arch Oral Biol* 8:523–550.

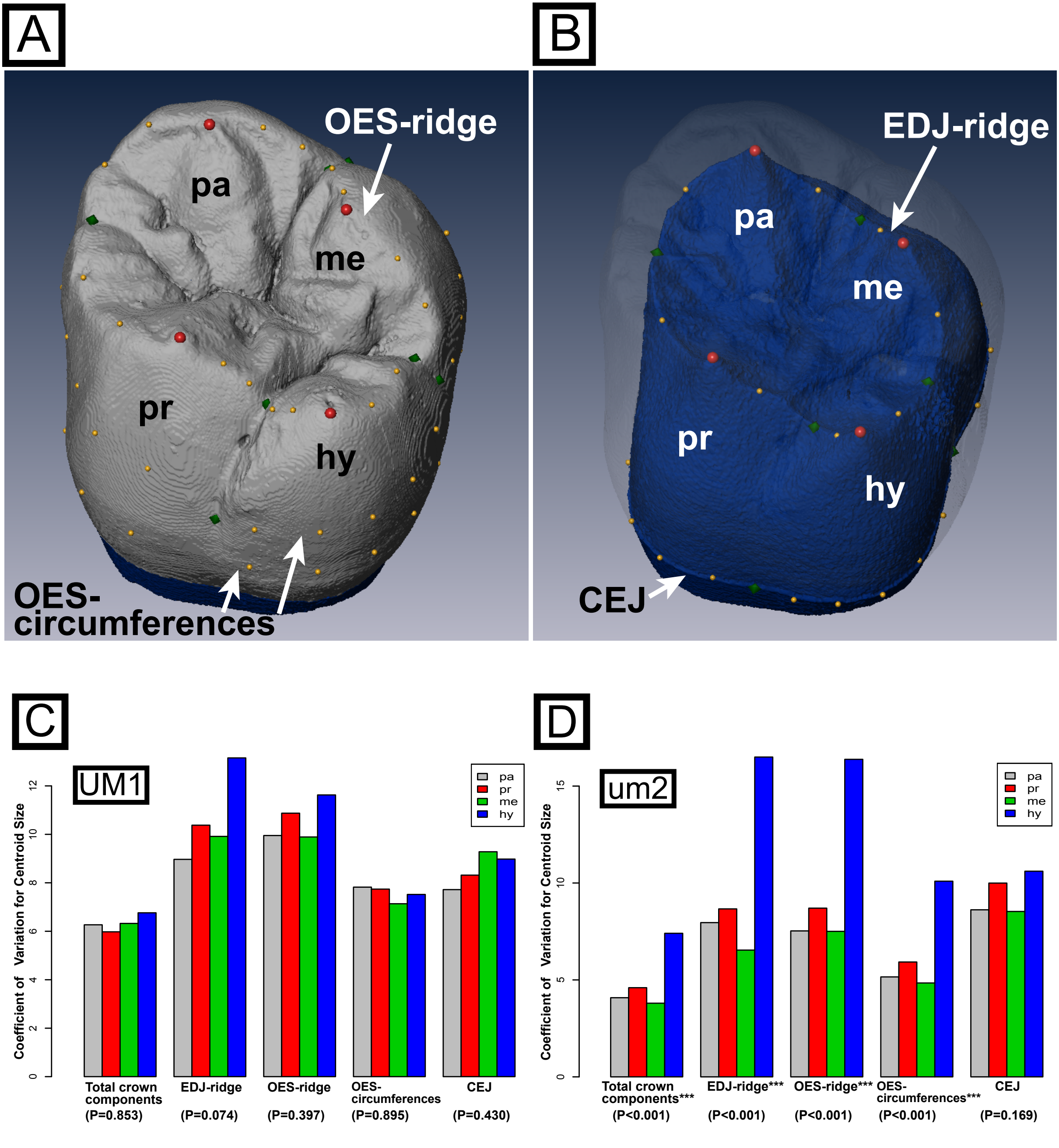
A
OES-ridge
pa
me
pr
hy
OES-
circumferences
B
EDJ-ridge
pa
me
pr
hy
CEJ
C
UM1
pa
pr
me
hy
Coefficient of Variation for Centroid Size
0
2
4
6
8
10
12
Total crown
components
(P=0.853)
EDJ-ridge
(P=0.074)
OES-ridge
(P=0.397)
OES-
circumferences
(P=0.895)
CEJ
(P=0.430)
D
um2
pa
pr
me
hy
Coefficient of Variation for Centroid Size
0
5
10
15
Total crown
components***
(P<0.001)
EDJ-ridge***
(P<0.001)
OES-ridge***
(P<0.001)
OES-
circumferences***
(P<0.001)
CEJ
(P=0.169)

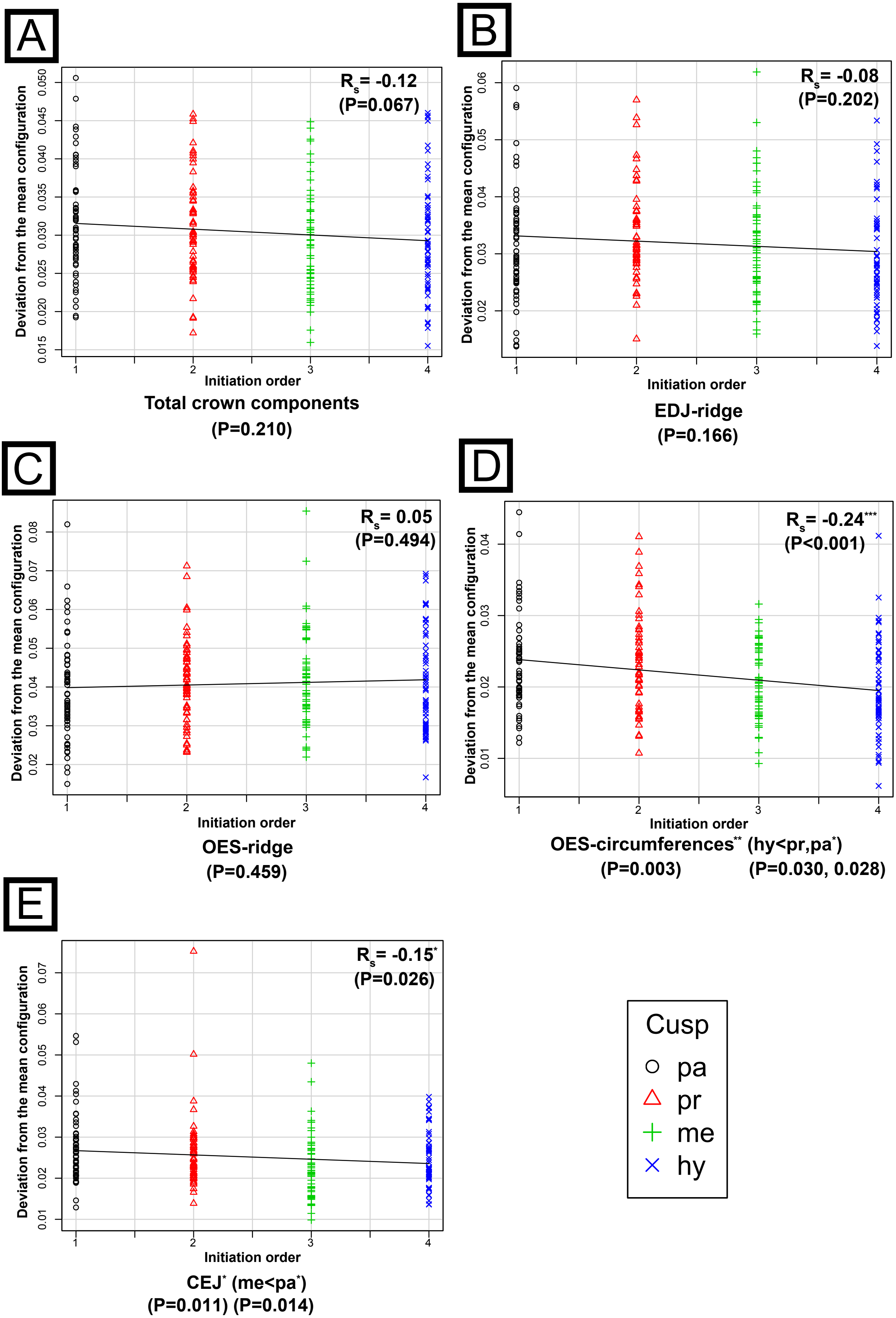
A
Rs= -0.12
(P=0.067)
Deviation from the mean configuration
Initiation order
Total crown components
(P=0.210)
B
Rs= -0.08
(P=0.202)
Deviation from the mean configuration
Initiation order
EDJ-ridge
(P=0.166)
C
Rs= 0.05
(P=0.494)
Deviation from the mean configuration
Initiation order
OES-ridge
(P=0.459)
D
Rs= -0.24***
(P<0.001)
Deviation from the mean configuration
Initiation order
OES-circumferences** (hy<pr,pa*)
(P=0.003) (P=0.030, 0.028)
E
Rs= -0.15*
(P=0.026)
Deviation from the mean configuration
Initiation order
CEJ* (me<pa*)
(P=0.011) (P=0.014)
Cusp
pa
pr
me
hy

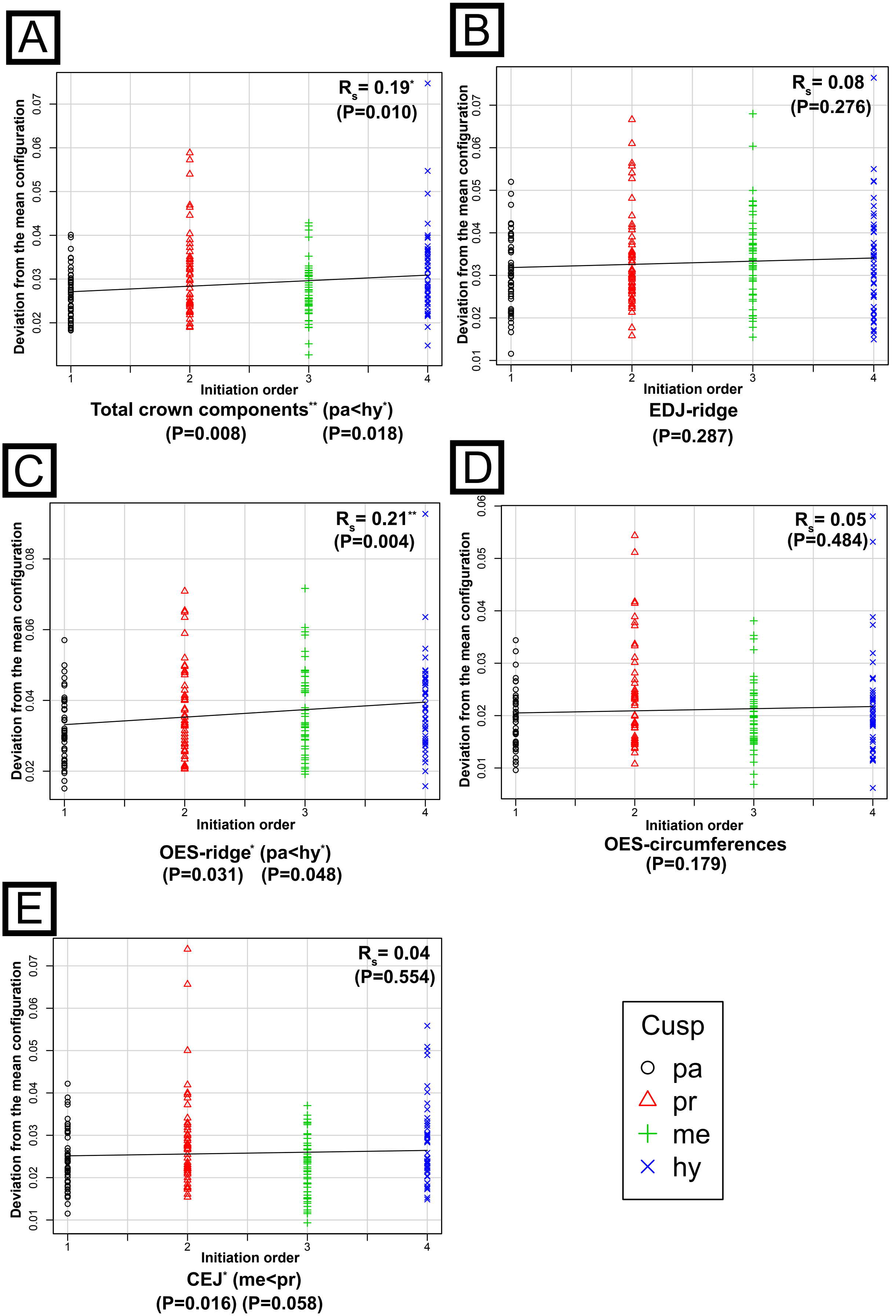
A
Deviation from the mean configuration
Initiation order
R$_s$= 0.19*
(P=0.010)
Total crown components** (pa<hy*)
(P=0.008) (P=0.018)
B
R$_s$= 0.08
(P=0.276)
EDJ-ridge
(P=0.287)
C
R$_s$= 0.21**
(P=0.004)
OES-ridge* (pa<hy*)
(P=0.031) (P=0.048)
D
R$_s$= 0.05
(P=0.484)
OES-circumferences
(P=0.179)
E
R$_s$= 0.04
(P=0.554)
CEJ* (me<pr)
(P=0.016) (P=0.058)
Cusp
pa
pr
me
hy

Supplementary Data

The cervical line of each tooth was manually traced using an interpolation curve tool to generate the best-fit plane. The tooth was then aligned so that this plane fit the *xy*-plane of the Cartesian coordinate system where the centroid of the cervical line defined the origin.

OES-ridge that connects adjacent cusp tips is separated at the lowest points (breakpoints) on which are located between the two cusps. The cusp tips and breakpoints divide the whole OES-ridge into eight sections. For each section, two semi-landmarks were set so that the ridge length is divided into equal one-thirds.

OES-circumferences (outlines) are traced at one-thirds and two-thirds of the height between the protocone tip and the cervical plane. Each circumference is divided into four sections (corresponding to the four cusp regions) by the inter-cuspal grooves. Ten semi-landmarks (the sum of five semi-landmarks of each circumference) are digitized in each section equi-angularly at the intersection of each OES-circumference with a plane perpendicular to the *xy*-plane passing through the origin.

The same procedure as used for the OES-ridge was performed on the dentin horn and EDJ-ridge, and the ridge length of each section is divided at the midpoint by one semi-landmark.

CEJ curve is also traced and divided into four sections at the most internally protuberant points between the adjacent two cusp regions. For each section, 5 semi-landmarks that divide the section into 6 parts equi-distantly are taken.

The number of semi-landmarks on the EDJ and the OES were determined to satisfy two criteria: 1) that each cusp has the same number of (semi)landmarks and 2) that the contributions of sections between (semi)landmarks to the curve are relatively equal to each other (Skinner et al., 2009;

Skinner and Gunz, 2010).

Each four crown component (EDJ-ridge, OES-ridge, OES-circumferences, CEJ) is divided into 4 cusp regions that span from breakpoint to breakpoint. Those breakpoints are not included in the subsequent analyses. Finally, the dataset was represented by four coordinate matrices comprising a total of 8 landmarks and 84 semi-landmarks (Supplementary Figure 1: 2 landmarks and 21 semi-landmarks for each of the four cusps).

Semi-landmarks are not considered to be homologous landmarks unless they are slid (Bookstein, 1997). The minimum bending energy algorithm (Bookstein, 1997; Gunz et al., 2005) was adopted. This data processing was performed by W. Y. using MATHEMATICA 8 (www. wolfram.com).

Centroid size (CS), defined as the square root of the summed squared distances of the coordinates from their centroid, of each cusp in the total and each crown component was calculated. Coefficient of variation (CV) of the CS of each cusp was used as a measure of size (not height) variability. For comparisons of shape variability among cusps, Generalized Procrustes Analysis (GPA) was repeated for the landmark set of the total and each crown component in order to include the information of relative spatial distribution among cusps. The square root of the sum of the squared distances between Procrustes transformed coordinates of each cusp and its landmark mean configuration was used as the measure of shape variability.

Figure legends

Supplementary Figure 1. Each four cusp delineation of maxillary permanent first molar crown (lingual view) is represented by landmarks connecting each other on the same crown component in a cusp. Landmarks, including semi-landmarks after slid, are represented by stars: on EDJ-ridge, triangles: on OES-ridge, circles: on OES-circumferences, squares: on CEJ. EDJ-ridge and OES-ridge are divided into four cusp regions by break points that are located at the lowest points between adjacent two dentin horns or cusp tips. Two OES-circumferences are traced at one-thirds and two-thirds of the height between the protocone tip and the cervical plane and divided into four sections, corresponding to the four cusp regions, by the inter-cuspal grooves. CEJ curve is divided into four sections at the most internally protuberant points between the adjacent two cusp regions. Each cusp has a total of 23 landmarks (2 landmarks and 21 semi-landmarks). pa, paracone; pr, protocone; me, metacone; hy, hypocone.

References

Bookstein FL (1997). Landmark methods for forms without landmarks: morphometrics of group differences in outline shape. *Med Image Anal* 1:225–243.

Gunz P, Mitteroecker P, Bookstein FL (2005). Semilandmarks in three dimensions. In: Modern Morphometrics in Physical Anthropology. Slice DE, editor. New York: Kluwer Academic/Plenum Publishers, pp. 73–98.

Skinner MM, Gunz P, Wood BA, Boesch C, Hublin J (2009). Discrimination of extant *Pan* species and subspecies using the enamel-dentine junction morphology of lower molars. *Am J Phys Anthropol* 140:234–243.

Skinner MM, Gunz P (2010). The presence of accessory cusps in chimpanzee lower molars is consistent with a patterning cascade model of development. *J Anat* 217: 245–253.

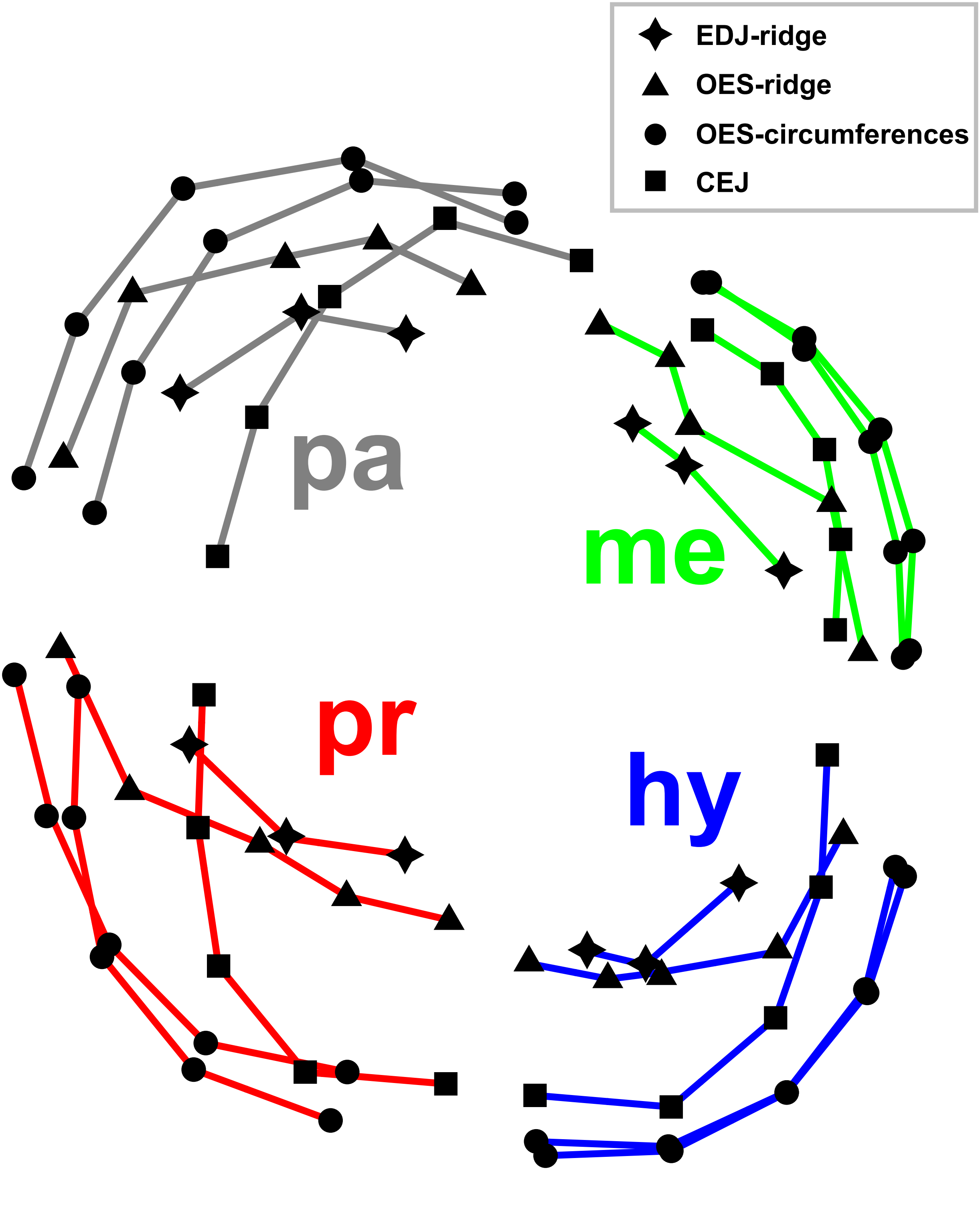
EDJ-ridge
OES-ridge
OES-circumferences
CEJ
pa
me
pr
hy